

The Age and Stellar Parameters of the Procyon Binary System

James Liebert¹, Gilles Fontaine², Patrick A. Young³, Kurtis A. Williams⁴, and David Arnett¹

Received _____; accepted _____

Accepted for ApJ, 15 Mar 2013

¹Department of Astronomy and Steward Observatory, University of Arizona, Tucson, AZ 85721, jamesliebert@gmail.com, darnett@as.arizona.edu

²Département de Physique, Université de Montréal, C.P. 6128, Succ. Centre-Ville, Montréal, Québec, Canada H3C 3J7, fontaine@astro.umontreal.ca

³School of Earth and Space Exploration, Arizona State University, Tempe AZ 85287, pyoung.3@asu.edu

⁴Texas A&M University, Commerce TX 75429, Kurtis.Williams@tamuc.edu

ABSTRACT

The Procyon AB binary system (orbital period 40.838 years, a newly-refined determination), is near and bright enough that the component radii, effective temperatures and luminosities are very well determined, although more than one possible solution to the masses has limited the claimed accuracy. Preliminary mass determinations for each component are available from HST imaging, supported by ground-based astrometry and an excellent *Hipparcos* parallax; we use these for our preferred solution for the binary system. Other values for the masses are also considered. We have employed the TYCHO stellar evolution code to match the radius and luminosity of the F5 IV-V primary star to determine the system’s most likely age as 1.87 ± 0.13 Gyr. Since prior studies of Procyon A found its abundance indistinguishable from solar, the solar composition of Asplund, Grevesse & Sauval ($Z=0.014$) is assumed for the HR Diagram fitting. An unsuccessful attempt to fit using the older solar abundance scale of Grevesse & Sauval ($Z=0.019$) is also reported. For Procyon B, eleven new sequences for the cooling of non-DA white dwarfs have been calculated, to investigate the dependences of the cooling age on (1) the mass, (2) the core composition, (3) the helium layer mass, and (4) heavy-element opacities in the helium envelope. Our calculations indicate a cooling age of 1.19 ± 0.11 Gyr, which implies that the progenitor mass of Procyon B was $2.59^{+0.44}_{-0.26} M_{\odot}$. In a plot of initial vs final mass of white dwarfs in astrometric binaries or star clusters (all with age determinations), the Procyon B final mass lies several σ below a straight line fit.

Subject headings: white dwarfs – stars: fundamental parameters (classification, colors, luminosities, masses, radii, temperatures, etc.) – stars: atmospheres

1. Introduction

Procyon A is the 14th nearest star and stellar system to the Sun, according to Henry (2011), at a distance of 3.51 parsecs or 11.46 light years – see van Leeuwen (2007). Its spectral type is F5 IV-V. Bessel (1844) discovered that the (large) proper motion of Procyon on the sky was perturbed by what he recognized to be an unseen companion. Procyon B was first detected visually at the end of the 19th century by Schaeberle (1896). The first recognition that the companion was like those in the Sirius and 40 Eri systems, later to be called white dwarfs, may be the work of the Irish amateur astronomer John Ellard Gore. However, he did not properly publish this result in the astronomical literature – see the discussions of his work by FitzGerald (1966) and Holberg (2009).

The first orbital elements were determined by Auwers (1862), who showed that the orbital period would be about 40 years. We now know that the more exact period is 40.838 years (H. E. Bond & G.H. Schaefer, 2012 private communication). Solar-like oscillations in Procyon A were first reported by Brown et al. (1991), and several authors have since investigated the structure and evolution of that star through a seismic approach (see, e.g., Dogan et al. 2010 and references therein). We come back to the asteroseismological properties of Procyon A in § 5.

Like Sirius A studied in Liebert et al. (2005, hereafter Paper I), Procyon A has an extremely accurate interferometric radius measurement, and an extremely accurate trigonometric parallax; the luminosity is also very accurate. Sirius A is certainly a main sequence star, while Procyon A could be entering or about to enter the subgiant branch. In contrast to the Sirius system, however, the astrometric mass solution for the Procyon system has been a controversial issue, as we shall discuss in § 2.

In comparison with the white dwarf Sirius B, Procyon B is very different from other (mostly DA) white dwarfs previously used for the problem of the star’s initial-to-final mass

relation (IFMR). Mainly it has a helium-dominated atmosphere polluted by heavy elements (DQZ spectral type), a lower mass, and a cooler temperature. The mass, radius and T_{eff} determined for the B component will be discussed in § 3.

In § 4 we address the atmospheric abundances of Procyon A and the interior abundances to be used for modelling in § 5. Here we employ the TYCHO stellar evolution code (Young & Arnett 2005) to fit the position of Procyon A in an HR diagram, and determine the age.

In § 6 eleven calculations of the cooling time of Procyon B are presented, for different assumptions about the mass, the helium envelope mass, and its composition. The cooling time is the length of time since the degenerate entered the white dwarf sequence; this has been used for the coolest white dwarfs to estimate ages of the Galactic disk (Liebert, Dahn, & Monet 1988) and halo (Hansen et al. 2007 – using the globular cluster NGC 6397). The difference between the systemic age and the white dwarf cooling time yields the best theoretical estimate of the initial mass of the white dwarf. Moreover, as discussed in § 6, Procyon B presents a complicated case for the calculation of the cooling age. Further remarks pertinent to this more challenging physical situation are discussed in that section.

This paper adds a valuable new object with accurately determined stellar parameters (masses, radii, luminosities) to the initial-to-final mass relation (IFMR) for progenitors and white dwarfs. The vast majority of other data points have white dwarfs with hydrogen-rich atmospheres, while Procyon B has a complicated helium-rich envelope and atmosphere. It is possible that the IFMR for helium-rich white dwarfs may differ from the hydrogen-rich distribution. We show in § 7 how Procyon B compares with Sirius B and white dwarfs in star clusters for which the IFMR of low to intermediate mass stars has been determined.

2. The Physical Parameters of Procyon A

As noted in the Introduction, a precise radius measurement is available for Procyon A, from measurements of the angular diameter with the ESO Very Large Telescope Interferometer. The radius is $R = 2.031 \pm 0.013 R_{\odot}$ or $\pm 0.65\%$ (Aufdenberg, Ludwig, & Kervella 2005). This radius value is based on the authors “best estimate” angular diameter of 5.404 ± 0.031 mas at 2.2μ . Note that the authors constructed model atmospheres for Procyon in three ways: (1) stand-alone one-dimensional (1D) PHOENIX structures, radiation fields, and spectra (Hauschildt et al. 1999); (2) CO⁵BOLD 3D structures temporarily and spatially averaged to 1D, then read by PHOENIX for computation of the corresponding radiation fields (Freytag et al. 2002); and (3) stand-alone 1D ATLAS 12 (Kurucz 1992) structures, radiation fields and spectra. Note that the quantitative assessment of the limb darkening, on which the radius value is determined, depends on the model atmospheres analysis. The authors discuss in detail their assessment of these different models, leading to their “best estimate”.

These authors also cite the earlier measurement on Mt. Wilson, California using the Mark III Interferometer at 500 and 800 nm (Mozurkewich et al 1991), whose limb-darkened value of the angular diameter (5.51 ± 0.05 mas) agrees marginally within the errors. Their new measurement compares to an older, slightly less accurate, but consistent value of $2.048 \pm 0.025 R_{\odot}$ by the same group (Kervella et al. 2004), which corresponds to an adopted angular diameter of 5.448 ± 0.053 mas. Casagrande et al. (2010) got a lower, less accurate, but consistent 5.326 ± 0.068 mas. For the radius (R_A) of the primary star in this paper, we adopt the Aufdenberg et al. (2005) best value. Note that the Kervella et al. and Aufdenberg et al. results differ by less than 1%. Adopting either one results in an essentially identical fit.

The *Hipparcos* satellite mission provided the precise measurement of the trigonometric

parallax of $0.28593 \pm 0.00088''$ (or $\pm 0.3\%$). Using the bolometric energy distribution and the effective temperature determination ($6,543 \pm 84$ K), the luminosity of Procyon A is determined in Aufdenberg et al. (2005) to be $\log L/L_{\odot} = +0.83 \pm 0.04$. Note that Chiavassa et al. estimate $T_{\text{eff}} = 6591$ K or 6556 K depending on how the bolometric flux is calculated, within the error bars of Aufdenberg et al. (2005). The former value differs the most from Aufdenberg et al.’s preferred 6543 K, resulting in $\log L/L_{\odot} = +0.843$ (with one more significant digit than is warranted). The difference between these two values hardly matters in Figure 1.

Two decades ago the mass of the “A” component was believed to be near $1.75 M_{\odot}$ (Irwin et al. 1992). However, main sequence evolutionary models at that mass were too luminous by a factor of two compared with the observed luminosity (Guenther & Demarque 1993). Long-term imaging by HST, combined with the interferometric radius and trigonometric parallax measurements cited above led to a great improvement in the stellar parameters. First, Girard et al. (2000) produced an improved astrometric solution based on analysis of 250 photographic plates spanning 83 years, augmented with early Hubble data. They found $M_A = 1.497 \pm 0.037 M_{\odot}$, almost exactly the $1.50 M_{\odot}$ predicted by Guenther & Demarque (1993).

The problem is that HST imaging has only been possible for only about half of the orbital period. The combining of space-based imaging and the much longer series of ground-based observations has often been fraught with difficulties. Apparent systematic offsets often occur in the respective measurements of the separations and position angles. Girard et al. (2000) found that, if they restricted the astrometric analysis to the excellent images obtained with the WFPC2 camera – i.e., with no ground-based data – a substantially lower mass ($1.465 M_{\odot}$) for Procyon A was the result. At that time HST imagery covered only about a decade.

Allende Prieto et al. (2002) revisited the Procyon A solution using the *Hipparcos* parallax and the stellar angular diameter by Mozurkevich et al. (1991) discussed previously. They derived the primary’s mass to be a much lower $1.42 \pm 0.06 M_{\odot}$. This is consistent with the ground-based Gatewood and Han (2006) value of the primary’s mass of $1.43 \pm 0.034 M_{\odot}$, determined from their Multichannel Astrometric Photometer **MAP** camera, built at the University of Pittsburg (Gatewood 1987). The **MAP** parallax is 286 ± 0.95 mas, which agrees well with the *Hipparcos* value.

Schaefer et al. (2006) reported a preliminary solution resulting from a Space Telescope Science Institute-led program to extend the imaging program on the Procyon binary orbit. Their result was in excellent agreement with the Girard et al. (2000) analysis including ground-based data. Several more years of HST data since 2006 now result in the following masses: $1.499 \pm 0.031 M_{\odot}$ for Procyon A and $0.553 \pm 0.022 M_{\odot}$ for Procyon B (G. H. Schaefer and H. E. Bond, 2012 private communication). This solution uses available HST data from 1995 through 2012 plus, appropriately weighted, the archival ground-based data.

It is not difficult to see how the total mass of the system is specified from accurate HST astrometry. Using Newton’s gravitational formula for Kepler’s third law, $(M_A + M_B) = a^3 / \pi^3 P^2$, with the semimajor axis (a) and period (P) well known, the sum of the masses is fixed at $2.052 M_{\odot}$. Ground-based observations of the wobble of the A component about the center-of-mass on the sky then fix a_A , $a_A + a_B = a$, and $M_A/M_B = a_B/a_A$. Thus the solution provides separate values for M_A and M_B .

The mass determinations remain a matter of dispute in the literature. We begin with $1.499 M_{\odot}$ as the HST-based, preferred mass of the primary for fitting in § 5. We also consider $1.42 M_{\odot}$ as a lower bound to the mass of the primary. Note that, in their recent analysis, Chiavassa et al. (2012) give arguments in favor of the $1.43 M_{\odot}$ Gatewood and Han value.

3. The Physical Parameters of Procyon B

Procyon B was first detected visually at the end of the 19th century by Schaeberle (1896), and was historically one of the first white dwarfs to be discovered. Even early estimates of the mass (M_B) of the white dwarf component, such as that by Strand (1951), showed that it is much closer to the mean value of field white dwarfs than is Sirius B. The updated Schaefer et al. HST solution gives $0.553 \pm 0.022 M_\odot$ for the mass of the secondary, and we consider this the benchmark value for M_B . To be sure this is much smaller than previous estimates for the secondary, such as $0.622 M_\odot$ (Irwin et al. 1992) and $0.602 \pm 0.015 M_\odot$ (Girard et al. 2000). Values in between these have been published. The Kervella et al. (2004) lower mass solution of $1.42 M_\odot$ for the primary led to $M_B = 0.575 \pm 0.017 M_\odot$ for B. The Gatewood and Han (2006) primary mass of $1.43 \pm 0.034 M_\odot$ resulted in $0.58 \pm 0.014 M_\odot$ for the secondary. To illustrate the dependence on mass, the cooling time for a mass of $0.602 M_\odot$ (Girard et al. 2000) is also discussed in § 6.

As mentioned in the Introduction, the nature of the “B” white dwarf poses additional problems. The atmosphere is helium-rich, with trace abundances of carbon, calcium, magnesium and iron, but no detection of hydrogen. This is an unusually diverse abundance pattern for a white dwarf atmosphere, and complicated greatly the determination of the atmospheric parameters. Not knowing of the complication, in the absence of an ultraviolet spectrum, Provencal et al. (1997) used pure hydrogen and helium atmospheres to model the spectral energy distribution. Preferring the helium fit due to its optical “DC” spectrum, they found $T_{\text{eff}} = 8,688$ K. This implied a stellar radius of $0.0096 \pm 0.0005 R_\odot$. Given the mass, this small radius implied that the interior composition of the white dwarf could not be carbon-oxygen, but rather something very dense like iron (Shipman & Provencal 1999). This conclusion was unsettling to stellar theorists.

Once the complicated ultraviolet spectrum was revealed with the Space Telescope

Imaging Spectrograph on the Hubble Space Telescope, Provencal et al. (2002) got themselves out of this “iron box”. Atmospheres with realistic trace abundances, obtained from fitting the spectrum and the 1,800–10,000Å spectral energy distribution were employed to obtain $T_{\text{eff}} = 7,740 \pm 50$ K. They now estimated the radius to be $0.01234 \pm 0.00032 R_{\odot}$, consistent with a carbon-oxygen interior. Note that Procyon B is the only white dwarf in a binary system or star cluster which does not have an atmosphere amenable to a mass determination from either the fitting of hydrogen or He I lines. It is also the coolest such white dwarf.

4. The Atmospheric and Interior Abundances of Procyon A

There is a long literature trail indicating that the Procyon A atmospheric abundance cannot be distinguished from solar. We cite five studies: Heiter & Luck (2003), and Luck & Heiter (2005), as part of a study of all bright, nearby stars in the Northern Hemisphere, analyzed Procyon A using high resolution spectra. They found an iron abundance $[\text{Fe}/\text{H}] = -0.04 \pm 0.06$. Valenti & Fischer (2005), as part of a systematic study of nearby stars using echelle spectra, obtained $[\text{Fe}/\text{H}] = -0.05 \pm 0.03$. In Allende Prieto et al.’s (2004) study of stars more luminous than $M_V = +6.5$ within 14.5 pc of the Sun, a value of $+0.08$ was determined for Procyon A. Finally, in the most comprehensive Geneva-Copenhagen study of solar neighborhood stars (Nordström et al. 2004), a value of $[\text{Fe}/\text{H}] = +0.05$ was reported. Both of the last two author groups discuss the possible systematic error due to the coupling of the $[\text{Fe}/\text{H}]$ determination to the error in the $\log g$ value. Note that Procyon A is cool enough that peculiar diffusion / gravitational support mechanisms should not distort the surface abundances from the interior abundance. There could, nevertheless, be a small diffusion of heavy elements out of the thin convective envelope.

However, recently there has been controversy about what the solar abundance actually

is. Inevitably, the abundance parameters to be run for the stellar evolution models of Procyon A, to be described next in § 5, must therefore be linked to this controversy, so a few comments are in order.

The newer solar abundance scale determined from 3D, non-LTE calculations of the solar atmosphere (Asplund et al. 2004, 2005, 2009 – the latter hereafter A09), and now Lodders 2010) have significantly lower abundances of oxygen, carbon and nitrogen than previous estimates (Grevesse & Sauval 1998). The abundance of neon is a particular problem, since it is impossible to measure this element in the Sun (or Procyon A), but is likely to be comparable numerically to the three elements mentioned previously. The overall heavy element abundance parameter for the Sun decreases to a primordial value of $Z=0.0153$.

The Asplund A09 scale has been challenged because it breaks the accord of the “standard solar” interior model with helioseismological measurements (Bahcall et al. 2005). A solar model with these abundances incorrectly predicts the depth of the convection zone, the depth profiles of sound speed and density, and the helium abundance (Basu & Antia 2004). As a check on the magnitude of likely systematic errors due to uncertainty in the actual solar (and Procyon A) abundance, we retain consideration of the older Grevesse & Sauval (1998) solar abundance which corresponds to $Z=0.019$.

5. The Fitting of Procyon A in a Radius-Luminosity “HR” Diagram

The TYCHO code – <http://chandra.as.arizona.edu/~dave/tycho-intro.html> – incorporates the most current microphysics for opacities, equation-of-state, and nuclear reactions. In particular, the code has been upgraded with an algorithm based on a physical analysis of 3D hydrodynamic simulations of convection, not an astronomically-calibrated

version of the mixing length theory. It includes non-locality and time dependence of flow, dynamical acceleration, turbulent dissipation, Kolmogorov heating, compositional effects and dynamically-defined boundary conditions (instead of parameterized overshooting schemes), all in a single, self-consistent formulation. The code is regularly tested against observations of double-lined eclipsing binaries and cluster isochrones to ensure consistency and accuracy. It produces superior fits to observational test cases without adjustment of parameters.

These changes make possible fits to nuclear-burning stars on the HR Diagram, especially those on or near the main sequence (Arnett, Meakin, & Young 2009, 2010). Robust, consistent ages for (nondegenerate) binary stars with well-determined luminosities, masses, radii and temperatures have been determined by Young et al. (2001), Young & Arnett (2005).

In additon to the mass, we have to input the abundance parameters Y and Z , where Z scales by the solar ratios of individual elements. Since we cannot regard the solar atmospheric abundance issue as fully resolved, we therefore have computed sequences using the Lodders (2010) value of $Z = 0.0153$ and also evaluated the older solar abundance of Grevesse and Sauval (1988) which imply $Z = 0.019$.

In Figure 1 we show evolutionary tracks for $Z = 0.0153$ of (1) $1.499 M_{\odot}$ (in black), the best value from preliminary HST astrometry (§ 2), fitting the correct luminosity and radius at age 1.74 Gyr; (2) $1.48 M_{\odot}$ (red) at 1.87 Gyr, the best fit to the luminosity (to three significant digits); (3) $1.463 M_{\odot}$ (green) at 1.99 Gyr; and (4) the lower $1.42 M_{\odot}$ (blue) at 2.51 Gyr favored by largely ground-based studies cited in § 2. The highest three masses fit within 1σ late on the main sequence. For $1.42 M_{\odot}$ the fit misses by more than 2σ late on the main sequence. Note that best-fit ages include the pre-MS evolution, without pre-MS accretion, but only the tracks from the beginning of the main sequence are shown here. We

also tried a fit with the Grevesse & Sauval (1998) $Z = 0.019$ abundance at $1.48 M_{\odot}$, but it is 1.45σ underluminous when it reaches the correct radius on the main sequence at age 1.96 Gyr. Given the evidence from A09 and Lodders (2010) that this solar metallicity value is too large, this marginal attempt at a fit is not shown in the figure.

We therefore believe that 1.87 ± 0.13 Gyr from the $1.48 M_{\odot}$ fit is the best estimate of the age of the binary system, with the uncertainty given by the bracketing age values for the 1.499 and $1.463 M_{\odot}$ fits. Note that Provencal et al. (2002) estimated the nuclear lifetime of 1.3 Gyr for component B, estimating $\sim 2.1 M_{\odot}$ as its progenitor mass. These authors use the cooling age from models of Wood (1995) for pure carbon cores – the only calculations available then. We now explore a range of alternative compositions for the white dwarf in § 6. Since our best-fit mass using the TYCHO models lies well within the error bars of the preliminary HST astrometric mass of $1.499 M_{\odot}$, we adopt $1.48 M_{\odot}$ as the preferred or “benchmark” mass of Procyon A.

Note that the fitting of a star with mass near $1.5 M_{\odot}$ at this stage of evolution presents uncertainties due to having both a small convective core and a small convective envelope. Due to the former, the main sequence lifetime is affected by the uncertainty in the amount of hydrogen fuel available for reactions in the core. Note that remaining uncertainties in the treatment of mixing beyond the convective core boundary, in the primordial solar abundance mix, or in any of the other model physics probably add larger systematic errors, by amounts which are difficult to quantify. The convective envelope leads to implied small differences between the interior and atmospheric Z abundances, as noted earlier.

For Kervella et al.’s (2004) similar analysis, the fit to the HRD parameters also occurs in a similar way. If $1.50 M_{\odot}$ is assumed, their fit is late on the main sequence at the much younger age of 1.3 Gyr. However, these authors assumed *no overshooting* of the convective core, i.e., less fuel, vs our calculations. For their preferred mass of $1.42 M_{\odot}$, the

corresponding fit is early in the H-shell burning phase at ages of 2.31–2.71 Gyr. This age range is close to what we achieve at $1.42M_{\odot}$ for which we determine an age of 2.51 Gyr (stated three paragraphs earlier), plotted as the blue track in Figure 1.

As indicated in the Introduction, stochastically excited p -modes have been observed in Procyon A since first reported by Brown et al. (1991), and several authors have attempted to exploit the seismic potential of that star using different data sets and models (e.g., Guenther & Demarque 1993; Barban et al. 1999; Chaboyer et al. 1999; Di Mauro & Christensen-Dalsgaard 2001; Eggenberger et al. 2005; Provost et al. 2006; Bonanno et al. 2007). However, their investigations have been limited by the accuracy of the detected pulsation frequencies. More recently, better data became available (Bedding et al. 2010) and have been modelled in a preliminary way by Dogan et al. (2010). We note that Dogan et al. (2010) report two possible seismic model for Procyon A, one of which characterized by a total mass of $1.50 M_{\odot}$ and an age of 1.83 Gyr (no uncertainties provided), which is remarkably close to our solution. We find this result most encouraging.

6. The cooling age and progenitor mass of Procyon B

6.1. White dwarf evolutionary sequences

The importance of the cooling age of a white dwarf was introduced in the Introduction. For Procyon B we first calculate the cooling time for a non-DA white dwarf of $M_B = 0.553 \pm 0.022 M_{\odot}$, the benchmark mass, but also evaluate the earlier alternative of $M_B = 0.602 M_{\odot}$ from Kervella et al. (2000). The fitted T_{eff} is $7,740 \pm 50$ K, as discussed in § 3. These error bars are the published, internal errors of the fit to the spectral energy distribution and absorption features, but are uncomfortably less than 1% of the value itself. For this object with a complicated DQZ spectrum, we feel more comfortable assuming

quadruple the formal T_{eff} error or ± 200 K.

There have unfortunately been a shortage of available evolutionary sequences for white dwarfs lacking thick hydrogen envelopes. Most cluster white dwarf studies in the last few decades have used the evolutionary models of Wood (1992, 1995), but always with an outer hydrogen layer. These calculations do include one sequence with no hydrogen, a “thin” helium envelope of 10^{-4} , atop a pure carbon core but with solar abundances of elements heavier than helium (Wood 2012, private communication). Hansen (1999) showed that pure helium envelope cooling models for $0.6 M_{\odot}$ by himself (for C, O and C/O cores) and by Salaris et al. (1997) cool considerably faster than the Wood sequence (see Hansen’s Fig. 7). Note that if a trace of heavy elements were assumed, the envelope opacity would be considerably increased. Hence, there has been some confusion as to what the cooling rates of white dwarfs lacking hydrogen layers should be. This issue is addressed in § 6.2.

For a cool, non-DA white dwarf with a simple, featureless spectrum, one could argue that the use of a pure-He envelope sequence such as from Hansen (1999) would yield the more robust cooling time. However, the spectrum of Procyon B shows the effects of (1) dredge-up of carbon from the diffusion tail of the core, with an atmospheric abundance $\log [\text{C}/\text{He}] = -5.5 \pm 0.2$ (Provencal et al. 2002); and (2) accretion of heavy elements – $\log \text{Mg}/\text{He} = -10.4$, $\log \text{Ca}/\text{He} = -12$, $\log \text{Fe}/\text{He} = -10.7$ with $\log \text{H}/\text{He} < -4$. Provencal et al. speculate that the secondary could be accreting a stellar wind from the primary at a rate of about $2 \times 10^{-19} M_{\odot} \text{ yr}^{-1}$. Thus, a calculation including additional opacity in the envelope layer may be more appropriate. Moreover, systematic errors need to be considered also due to the uncertain mix of carbon and oxygen in the core, and the thickness of the helium envelope. For this purpose one of us (GF) has calculated a new set of cooling tracks to estimate these errors and parameter dependences, and hopefully thus bound the possible cooling time of this white dwarf.

Salaris et al. (1997) explored the dependence of cooling rates on the internal chemical distribution of carbon and oxygen in the core. For their best choices of the combined effect of convective mixing and the $^{12}\text{C}(\alpha,\gamma)^{16}\text{O}$ reaction rate, carbon-oxygen profiles showing an enhancement of oxygen in the central regions are obtained for all white dwarf masses. Mass fractions of ^{16}O as high as 0.8 are found near $0.6 M_{\odot}$. This fraction declines with increasing core mass because the above reaction rate is highest at the lower core temperatures characteristic of lower masses. Thus, a core composition dominated by oxygen, or at least a mixture of carbon and oxygen, is more likely than one of pure carbon for Procyon B. Sequences have been calculated for pure oxygen, pure carbon, and for mixtures of carbon and oxygen according to the mass-dependent and depth-dependent results of Salaris et al. (1997). We pick the last of these three types of sequences as the benchmark core composition.

The cooling time also depends on the thickness of the helium layer. The helium-rich atmospheric composition indicates that some of the helium layer mass could have been lost in a late helium-shell flash that disposed of all of the hydrogen (Iben 1984). Values in the literature that have been considered include masses between 10^{-2} and $10^{-4}M_{\odot}$. The atmospheric carbon abundance is a strong constraint, since this results from dredgeup of the diffusion tail of carbon from the core. The study (Fontaine & Brassard 2005) fitting dredgeup models to match the spectra of Procyon B and a sequence of field DQ white dwarfs by Dufour, Bergeron, & Fontaine (2005) shows that the atmospheric carbon abundance of Procyon B favors a layer mass thickness of $\log M_{\text{He}}/M_{\odot} \sim -2.5 \pm 0.5$ (see their Fig. 12). We therefore consider this value as the benchmark, with sequences also calculated for a reasonable range of -2.0 and -3.0 .

Finally, it is very difficult to estimate the opacities due to elements heavier than helium in the partially-degenerate helium layer. This will depend on how deeply the heavy

elements have diffused into the envelope below the convection zone. In principle the carbon abundance profile can be calculated for the helium envelope from diffusion theory, with the atmospheric abundance as a surface boundary. To consider this dependence in an approximate way, sequences with $Z=0.001$ and $Z=0$ have been calculated, with the former as the benchmark while the latter is contradicted by the observation of carbon and heavier elements in the spectrum.

In Table 1, the cooling ages for the parameters of Procyon B are listed for 8 sequences at the favored mass of $0.553 M_{\odot}$, two for values at $\pm 0.022 M_{\odot}$, and one for the alternative $0.602 M_{\odot}$ (Girard et al. 2004). Also listed for each sequence are the core composition (C, O, or a more realistic Salaris C/O mix), the helium layer mass (-2.5 ± 0.5 as discussed earlier), and the heavy element abundance $Z=0.001$ or 0. All assume zero hydrogen abundance.

The benchmark cooling age of Procyon B is given by the model for $0.553 M_{\odot}$, with C/O core, $\log M(\text{He})/M = -2.5$, and $Z = 0.001$ in the envelope (benchmark parameters). The cooling value is 1.187 Gyr, with a formal, internal error of ± 0.104 Gyr due to uncertainties in the assumed effective temperature and the assumed mass. According to Table 1, a range of ± 200 K about the estimated effective temperature of $T_{\text{eff}} = 7740$ K translates into an age uncertainty of ± 0.085 Gyr, while a range of $\pm 0.022 M_{\odot}$ about the benchmark mass of $0.533 M_{\odot}$ translates into an age interval of ± 0.061 Gyr. Added in quadrature, these uncertainties lead to ± 0.104 Gyr. In addition, two sources of systematic error should be considered here. The age difference between a mixed (C/O) and a pure oxygen core is relatively small at 0.010 Gyr. For its part, uncertainty due to variations in the helium layer mass is ± 0.043 Gyr. Added again in quadrature with the above internal error, these systematic effects lead to a total uncertainty of ± 0.113 Gyr on the age. So we reach the value of 1.19 ± 0.11 Gyr for the white dwarf cooling time of Procyon B.

On the other hand, the $Z = 0$ envelope sequence with otherwise benchmark assumptions

yields a considerably larger age of 1.391 Gyr. Since this is inconsistent with ultraviolet observations of carbon and heavy elements in the ultraviolet spectrum, we consider a metal-free envelope an unrealistic assumption. Note that the atmospheric values determined by Provencal et al. (2002) already have a heavy element abundance (dominated by carbon) of $Z \sim 0.00001$. This parameter increases greatly below the convection zone throughout the partially-degenerate helium envelope (following profile of carbon dredge-up), until it reaches the C/O core.

Likewise, we do not consider the assumption of a pure carbon core realistic. The combination of a pure carbon core with zero metallicity envelope yields an even larger cooling age of 1.557 Gyr. The cooling age listed for the alternative mass of $0.602 M_{\odot}$, assuming benchmark values of the other parameters above, is 1.406 Gyr. A mass this large for the secondary disagrees by more than 2σ from that derived from HST astrometry and we no longer consider it in the rest of this paper. These several possibilities in this paragraph are not factored into the error bars in the preceding paragraph.

The difference between the age of the Procyon system and the cooling time of the white dwarf component, 0.68 ± 0.17 Gyr, corresponds to the sum of the pre-main sequence lifetime and the main sequence lifetime (plus the much shorter red giant phases) of the Procyon B progenitor. Using again our TYCHO evolutionary code, we thus find that the initial mass (M_i) of the secondary is $2.59_{-0.18}^{+0.22} M_{\odot}$, if the envelope Z value is fixed at 0.001. However, if one allows for the extreme upper limit to the cooling time from the assumption of $Z(\text{env}) = 0$, the error bars for the progenitor mass increase to $_{-0.26}^{+0.44} M_{\odot}$. The quoted errors on M_i are the quadrature sums of $-0.21, +0.40$ due to the uncertainty in the cooling time of the white dwarf, and $-0.16, +0.20$ due to systematic error in the age of the binary system (Table 2). In Figure 2, discussed in detail in the next section, the solid horizontal error bars for Procyon B are for the case of $Z(\text{env})$ fixed at 0.001, the extended light error

bars reflect the increase in cooling time for the limiting case $Z(\text{env}) = 0$.

6.2. Remarks on the dependence of the cooling rate on the envelope opacities

It may be worthwhile at this point to attract the attention of the reader on some subtleties of white dwarf cooling which leave their signature on the data presented in Table 1. For instance, as is well known (and revealed again in the table), pure C core models systematically cool slower than models having cores made of heavier elements, all other things being the same. That a pure carbon core takes longer to cool is well understood, because the thermal energy in a given mass is locked up in more nucleons than for pure oxygen or a mixture. However, that the $Z = 0$ envelope takes longer to cool than one with heavy elements is not so intuitive, because one might think that the more opaque envelope with heavy elements would let the interior energy out more slowly. Our calculations show that cooling proceeds in two phases. At first the less opaque model does let the thermal energy escape more quickly, and core temperature decreases more rapidly. Despite this, however, the decrease in luminosity has to be slower for the less opaque model because of that extra energy that is made available to fuel the luminosity. Hence, in a first phase, the less opaque model actually cools *more slowly* to a given luminosity or T_{eff} . However then, after the less opaque star has let more of its thermal energy escape, there is no turning back and the price to pay, in a second phase, is that it will now cool *faster* the rest of the way than its more opaque counterpart. In the case of Procyon B at $T_{\text{eff}} = 7,740$ K, it is still warm enough to be in the first phase of that “relative” cooling and, hence, this is why the cooling age is larger for the less opaque model. If the star had a T_{eff} of $\sim 5,000$ K, then indeed the cooling age based on the less opaque envelope sequence would be shorter than than of the more opaque, as the conventional wisdom would expect. These arguments may be discerned from a careful perusal of Section III(a), subsection (ii) of Tassoul, Fontaine

and Winget (1990), although this discussion compares an opaque envelope of hydrogen with less opaque counterparts.

7. Procyon B and the Initial to Final Mass Ratio (IFMR)

As discussed in the last paragraph of the Introduction, the initial-to-final mass relation (IFMR) for progenitors and white dwarfs is fundamental in understanding a stellar population. This study of Procyon adds a data point near the low mass end with well determined stellar parameters; it may be valuable for testing whether differences exist in the IFMR for the distributions of hydrogen and helium-rich atmosphere white dwarfs.

Table 2 lists final (M_f) and initial (M_i) masses in M_\odot , cooling times (log in years), and estimated errors, first for Procyon B and Sirius B. The remaining data points come from white dwarfs found in Galactic star clusters, in order of increasing age (see footnotes). The collective data set is shown in Figure 2. Again, the age of the population is obtained generally from fitting the main sequence turnoff of the cluster color-magnitude diagram.

As given in Ferrario et al. (2005), the errors in M_i fall into two categories – observational (obs) or random, and systematic (sys), as listed in Table 2. The observational errors devolve from uncertainties in the M_f from fitting the Balmer lines (or, in one case, He I lines); the systematic errors come from uncertainties in the cluster or binary system age. Since the nuclear lifetime of the progenitor is the difference between the systemic age and the white dwarf cooling time, M_i depends on the age as well. Note that the uncertainties in the age determinations for the young clusters lead to large error bars in the estimates of the initial masses M_i .

We add GD 50 to the Pleiades “moving group”, since Dobbie et al. (2006) make a strong case based on astrometric and spectroscopic data that this ultramassive white dwarf

is associated with the star formation event that created the Pleiades cluster. They argue that it evolved as a single star from a progenitor of $6.3 M_{\odot}$, and that this may represent the first observational evidence that single-star evolution can produce white dwarfs with, in this case, a mass of $1.27 M_{\odot}$ (Bergeron, Saffer, & Liebert 1992) or $1.2(+0.07, -0.08) M_{\odot}$ (Bergeron et al. 1991). They make a weaker case that the massive white dwarf PG 0136+251, $1.20 \pm 0.03 M_{\odot}$ (Bergeron, Saffer, & Liebert 1992), may also be related to the Pleiades. However, information is lacking on the total (UVW) space motion of this object, so we do not include it here. We adopt an age of 125 ± 25 Myr for the Pleiades, which depends on the treatment of the convective core. This excludes a systematic uncertainty to the age which will be true for all clusters with main sequence turnoff stars of mass above $\sim 1.3 M_{\odot}$.

Williams, Bolte, & Koester (2004, 2009) present studies of white dwarfs in the cluster NGC 2168 (M35); this work supercedes the data listed in Ferrario et al. (2005). In the updated listing, 2168-22 is excluded since it is likely magnetic, and the weak Balmer lines could not be fit by the authors. The age of the cluster is believed to be 175 ± 50 Myr (Sung and Bessell 1999, von Hippel 2005).

For NGC 3532 (age 300 ± 25 Gyr) we take the view that the analysis with one of the 8.2 m VLT telescopes by Dobbie et al. (2009b) supercedes the earlier ESO observations of Koester & Reimers (1993). For NGC 2099 (age 490 ± 70 Myr), we note that star 2099-14 at $0.45 \pm 0.08 M_{\odot}$ likely has a helium core, implying formation from binary star evolution. A new white dwarf in the 500 ± 100 Myr Coma Berenices open cluster (Melotte 111), called 1216+260, has been studied by Dobbie et al. (2009a). Based on assuming a CO core and a thick H layer for this DA, they calculate the parameters listed in Table 2.

For the Praesepe and Hyades clusters, likely members of the Hyades “moving group” (Eggen 1958, Zuckerman & Song 2004), we adopt as the age 625 ± 50 Myr. The white

dwarfs from the Hyades were studied by Claver et al. (2001) and Ferrario et al. (2005). The only DB star among the cluster white dwarfs used here is 0437+138 in the Hyades. The Praesepe cluster stars were studied by Claver et al. (2001), Ferrario et al. (2005), Dobbie et al. (2004), and Casewell et al. (2009). For objects in common between these last two papers with many common authors, we adopt the values of the last paper, since the results were obtained with the UVES spectrograph on the VLT UT2. We omit 0837+218 since Casewell et al. (2009) make a good case that this is not a cluster member.

White dwarfs in older clusters overlapping and exceeding the likely age of Procyon have been analyzed and published since the Ferrario et al. work. For the older clusters (as well as Procyon B and Sirius B), the errors for M_i are relatively smaller.

Kalirai et al. (2008) identified four likely members of the open cluster NGC 7789, with age 1.40 ± 0.14 Gyr, and found two likely member white dwarfs in NGC 6819 with age 2.50 ± 0.25 Gyr. We note that the signal-to-noise ratio of the spectra with fitted Balmer lines are low compared to P. Bergeron’s usual standards; we quote the listed errors here. Kalirai et al. (2007) analyzed a number of the brightest white dwarfs in the very old Galactic cluster NGC 6791 (8.5 ± 1.0 Gyr); however, only 6791-7 was the only likely member not having a very low mass determination and likely helium core. The authors note that enhanced mass loss in the red giant phase, which is the likely origin of the helium white dwarfs, probably also occurred in this object, despite the fact that it retained a hydrogen atmosphere.

Finally, Kalirai et al. (2009) analyze a number of white dwarfs at the tip of the observed sequence in the globular cluster Messier 4. This is of course a Population II system with $[\text{Fe}/\text{H}] = -1.10 \pm 0.01$ (Mucciarelli et al. 2011), and likely age of 12.7 ± 0.7 Gyr (Hansen et al. 2002). The basic conclusion is that the $\sim 0.8 \pm 0.05 M_\odot$ stars now producing white dwarfs which have evolved to approximately $0.53 \pm 0.01 M_\odot$ (but we list the individual

determination for each of the latter).

Procyon B has a final mass below nearly all others of similar initial mass. It is one of only two white dwarfs here with a helium atmosphere. The other is the DB in the Hyades mentioned earlier, which has a mass similar to the other DA stars in that cluster and the Praesepe. The dashed line plots the simple linear relation from Ferrario et al. (2005) based on a fit to white dwarfs in more massive clusters available at that time. The Procyon B point lies more than $0.1 M_{\odot}$ or several σ below this line in the sense of having a lower final mass.

We should note that the close, cool double-DC binary G 107-70AB (Harrington, Christy, & Strand 1981) appears to be a similar situation at first glance. It was barely resolved from ground-based imaging at the U.S. Naval Observatory, Flagstaff Station. It is no surprise that this old result is superceded by 13 years of HST imaging (1995.8-2008.8), as of the latest fit – Schaefer et al. (2006, and private communication). The preliminary period is 18.546 ± 0.082 years, $a = 0.666''$, and $M_{tot} = 1.191 \pm 0.057 M_{\odot}$ (using the Hipparcos parallax of $0.0896 \pm 0.0014''$). Since only a small difference in magnitude between the two components is indicated, this suggests two components each of not quite $0.6 M_{\odot}$.

Using the integrated light from the two stars, Bergeron, Ruiz, & Leggett (1997) estimate 4900 K, $\log g = 7.35$, and their broad-band *BVRIJHK* energy distribution fits an H-rich atmosphere. That is, the spectrum would have been type DA if the temperatures of the two stars were warmer. The HST astrometry above suggests two white dwarfs each of mass near the well known peak of the DA mass distribution (Koester, Schulz, & Weidemann 1979). Note that the $\log g$ value inferred above is incorrect, since the method used by Bergeron et al. (1997) to estimate a surface gravity assumes a single star. Thus G 107-70AB are not cooler analogs of Procyon B.

We have no explanation for why the Procyon B remnant appears so undermassive vs

the initial mass we have derived. Suppose that virtually all of the helium envelope of the Procyon B nuclear progenitor could have been lost in the event (late helium-shell flash?) that also removed all of the hydrogen. However, stellar models of the asymptotic giant branch phase show that the maximum helium envelope mass remaining would have been only $\sim 0.01M_{\odot}$ if left intact.

Thus the loss of the entire helium envelope fails to account for the total mass shortfall by an order of magnitude. Rather, the evolution of the (presumably) carbon-oxygen core was evidently truncated before it could build up to a more normal mass for a single star with the indicated initial mass. The dilemma suggests that close binary evolution may have been involved, but the existing binary consists of two stars in an elliptical orbit of long period.

Hence, we are left with an interesting problem in (binary) stellar evolution. Note that there are still rather few stars analyzed from Population I clusters of age older than or similar to Procyon. In the future the numerous white dwarfs in the old disk clusters M 67 and NGC 188 will make useful additions to round out the low mass end of such a diagram.

We gratefully acknowledge Gail Schaefer of the CHARA array at Georgia State University, and Howard E. Bond of STScI, for allowing us to quote preliminary HST results which fix the masses of Procyon A and B, and for results on G 107-70AB. This work was originally supported by the National Science Foundation through grant AST-0307321 (JL and KAW). GF wishes to acknowledge the contribution of the Canada Research Chair Program.

Table 1. Parameters of Cooling Models at $T_{\text{eff}} = 7,940$ K, 7,740 K, and 7,540 K

ID	Core	$\log M_{\text{He}}/M$	Z	M/M_{\odot}	$\log g$	R/R_{\odot}	Age (Gyr)
					7.9676	0.012777	1.1069
1	C/O	-2.5	0.001	0.553	7.9681	0.012768	1.1870
					7.9687	0.012760	1.2772
					7.9297	0.013077	1.0516
2	C/O	-2.5	0.001	0.531	7.9303	0.013068	1.1274
					7.9309	0.013059	1.2122
					8.0045	0.012485	1.1650
3	C/O	-2.5	0.001	0.575	8.0050	0.012479	1.2501
					8.0055	0.012471	1.3438
					7.9637	0.012834	1.2336
4	C	-2.5	0.001	0.553	7.9642	0.012826	1.3236
					7.9648	0.012817	1.4251
					7.9709	0.012728	1.0992
5	O	-2.5	0.001	0.553	7.9714	0.012720	1.1770
					7.9720	0.012712	1.2650
					7.9730	0.012696	1.2962
6	C/O	-2.5	0.0	0.553	7.9736	0.012688	1.3914
					7.9742	0.012680	1.4990
					7.9693	0.012752	1.4500
7	C	-2.5	0.0	0.553	7.9699	0.012743	1.5573
					7.9705	0.012734	1.6774
					7.9762	0.012651	1.2634
8	O	-2.5	0.0	0.553	7.9767	0.012643	1.3544
					7.9772	0.012635	1.4565
					7.9661	0.012798	1.0705

Table 1—Continued

ID	Core	$\log M_{\text{He}}/M$	Z	M/M_{\odot}	$\log g$	R/R_{\odot}	Age (Gyr)
9	C/O	−2.0	0.001	0.553	7.9667	0.012790	1.1488
					7.9673	0.012781	1.2374
					7.9687	0.012756	1.1521
10	C/O	−3.0	0.001	0.553	7.9692	0.012747	1.2347
					7.9698	0.012739	1.3266
					8.0485	0.012145	1.3120
11	C/O	−2.5	0.001	0.602	8.0489	0.012138	1.4063
					8.0494	0.012132	1.5112

Table 2. Final – Initial Mass (M_f/M_i) Determinations

Star Name	M_f	dM_f	$\log \tau$	$d\log\tau$	M_i	$\pm dM_i(obs)$	$\pm dM_i(sys)$	Ref
Procyon B	0.553	0.022	9.075	0.074	2.59	0.21,0.40	0.16,0.20	1
Sirius B	1.000	0.020	8.091	0.020	5.056	0.171,0.262	0.213,0.273	2
LB 1497	1.023	0.026	7.781	0.062	6.542	0.346,0.458	0.866,1.614	3
GD 50	1.264	0.017	7.785	0.045	6.3	2.5,0.8	–,–	4,5
NGC 2516-1	0.931	0.098	7.760	0.230	5.411	1.017,0.500	0.524,0.386	6
NGC 2516-2	1.004	0.058	7.621	0.179	5.096	0.406,0.239	0.415,0.311	6
NGC 2516-3	0.969	0.039	7.922	0.079	6.141	0.692,0.427	0.924,0.587	6
NGC 2516-5	1.054	0.063	7.883	0.136	5.902	0.986,0.524	0.786,0.514	6
NGC 2168-1	0.873	0.091	7.228	0.260	4.39	0.23,0.09	0.35,0.27	7
NGC 2168-2	1.015	0.067	7.657	0.202	4.79	0.47,0.26	0.46,0.36	7
NGC 2168-5	0.916	0.075	6.103	0.088	4.21	0.00,0.00	0.29,0.23	7
NGC 2168-6	0.877	0.096	6.077	0.082	4.21	0.00,0.00	0.29,0.23	7
NGC 2168-11	0.802	0.096	8.047	0.173	6.63	0.00,1.38	1.89,0.96	7
NGC 2168-12	0.922	0.092	7.314	0.281	4.43	0.30,0.13	0.36,0.27	7
NGC 2168-14	1.010	0.072	7.865	0.167	5.32	0.95,0.44	0.73,0.48	7
NGC 2168-15	0.888	0.088	7.551	0.236	4.63	0.38,0.22	0.41,0.32	7
NGC 2168-27	1.022	0.072	7.840	0.170	5.22	0.71,0.42	0.68,0.45	7
NGC 2168-29	0.882	0.078	7.331	0.235	4.44	0.23,0.12	0.36,0.28	7
NGC 2168-30	1.011	0.122	7.808	0.289	5.12	1.49,0.55	0.63,0.43	7
NGC 2287-2	0.910	0.040	7.908	0.075	4.450	0.580,0.380	–,–	8
NGC 2287-5	0.910	0.040	7.964	0.071	4.570	0.640,0.430	–,–	8

Table 2—Continued

Star Name	M_f	dM_f	$\log \tau$	$d\log\tau$	M_i	$\pm dM_i(obs)$	$\pm dM_i(sys)$	Ref
NGC 3532-1	0.86	0.04	7.778	0.095	3.830	0.18,0.15	–,—	9
NGC 3532-5	0.820	0.04	7.580	0.115	3.71	0.150,0.130	–,—	9
NGC 3532-9	0.760	0.04	7.00	0.113	3.57	0.12,0.11	–,—	9
NGC 3532-10	0.96	0.04	8.173	0.060	4.58	0.47,0.33	–,—	9
NGC 2099-2	0.69	0.10	7.961	0.165	2.76	0.08,0.05	0.162,0.201	10
NGC 2099-3	0.76	0.13	8.190	0.190	2.92	0.16,0.14	0.197,0.258	10
NGC 2099-4	0.87	0.15	8.428	0.217	3.02	0.26,0.19	0.324,0.495	10
NGC 2099-5	0.83	0.14	8.271	0.188	3.02	0.26,0.19	0.219,0.305	10
NGC 2099-7	0.88	0.19	8.378	0.289	3.26	0.78,0.40	0.278,0.405	10
NGC 2099-9	0.61	0.05	8.268	0.067	2.97	0.06,0.07	0.218,0.302	10
NGC 2099-10	0.74	0.04	8.090	0.068	2.81	0.04,0.02	0.178,0.225	10
NGC 2099-11	0.96	0.06	8.149	0.095	2.86	0.07,0.07	0.188,0.242	10
NGC 2099-12	0.55	0.07	8.394	0.126	3.30	0.30,0.22	0.290,0.429	10
NGC 2099-13	0.79	0.05	8.229	0.074	2.93	0.06,0.07	0.207,0.278	10
NGC 2099-14	0.45	0.08	8.487	0.085	3.31	0.20,0.26	0.400,0.674	10
NGC 2099-16	0.83	0.06	8.689	0.082	5.20	7.0,1.20	3.737,—	10
1216+260	0.90	0.04	8.560	0.052	4.77	0.97,5.37	–,—	11
0352+098	0.719	0.030	8.270	0.046	3.094	0.045,0.052	0.114,0.134	12
0406+169	0.806	0.031	8.488	0.046	3.465	0.109,0.147	0.172,0.225	12
0421+162	0.680	0.031	7.970	0.055	2.892	0.020,0.023	0.090,0.103	12
0425+168	0.705	0.031	7.549	0.077	2.789	0.011,0.010	0.079,0.088	12

Table 2—Continued

Star Name	M_f	dM_f	$\log \tau$	$d\log \tau$	M_i	$\pm dM_i(obs)$	$\pm dM_i(sys)$	Ref
0431+125	0.652	0.032	7.752	0.068	2.825	0.014,0.017	0.083,0.093	12
0437+138	0.740	0.060	8.470	0.047	3.663	0.030,0.030	–,–	13
0438+108	0.684	0.031	7.203	0.060	2.757	0.003,0.004	0.076,0.084	12
0833+194	0.721	0.043	8.431	0.049	3.32	0.33,0.22	–,–	14
0836+197	0.909	0.030	8.136	0.049	2.981	0.031,0.035	0.101,0.115	15
0836+199	0.831	0.037	8.612	0.069	3.997	0.350,0.652	0.297,0.428	15
0836+199	0.752	0.044	8.489	0.049	3.46	0.43,0.27	–,–	14
0836+201	0.620	0.031	8.154	0.050	2.993	0.028,0.046	0.102,0.117	15
0837+185	0.804	0.044	8.504	0.050	3.50	0.48,0.29	–,–	14
0837+199	0.819	0.032	8.351	0.048	3.194	0.081,0.062	0.153,0.129	15
0837+199	0.737	0.043	8.253	0.052	3.07	0.20,0.15	–,–	14
0840+190	0.849	0.045	8.566	0.050	3.73	0.71,0.39	–,–	14
0840+200	0.761	0.033	8.522	0.045	3.572	0.186,0.129	0.255,0.196	15
0840+200	0.721	0.043	8.420	0.048	3.30	0.32,0.21	–	14
0843+184	0.823	0.045	8.530	0.051	3.59	0.55,0.33	–,–	14
NGC 7789-4	0.560	0.020	8.061	0.032	2.080	0.080,0.080	–,–	16
NGC 7789-5	0.600	0.030	6.903	0.055	2.020	0.070,0.140	–,–	16
NGC 7789-6	0.720	0.030	8.204	0.045	2.100	0.090,0.090	–,–	16
NGC 7789-8	0.640	0.040	7.462	0.080	2.020	0.090,0.110	–,–	16
NGC 6819-6	0.530	0.020	7.591	0.035	1.600	0.060,0.050	–,–	17
NGC 6819-7	0.560	0.020	8.155	0.034	1.620	0.070,0.050	–,–	17

Table 2—Continued

Star Name	M_f	dM_f	$\log \tau$	$d\log \tau$	M_i	$\pm dM_i(obs)$	$\pm dM_i(sys)$	Ref
NGC 6791-7	0.530	0.020	8.176	0.060	1.160	0.040,0.030	–,–	18
M 4-0	0.520	0.040	7.602	0.070	0.800	0.050,0.050	–,–	19
M 4-4	0.500	0.030	7.279	0.024	0.800	0.050,0.050	–,–	19
M 4-6	0.590	0.040	7.255	0.050	0.800	0.050,0.050	–,–	19
M 4-15	0.550	0.040	7.322	0.043	0.800	0.050,0.050	–,–	19
M 4-20	0.510	0.050	7.690	0.075	0.800	0.050,0.050	–,–	19
M 4-24	0.510	0.030	7.204	0.028	0.800	0.050,0.050	–,–	19

Note. — (1) Procyon, 1.87 Gyr, this paper; (2) Sirius, 237.5 ± 12.5 , Liebert et al. (2005); (3) The Pleiades, 125 ± 25 Myr, Claver et al. (2001); (4) The Pleiades, 125 ± 25 Myr, Bergeron et al. (2002); (5) The Pleiades, 125 ± 25 Myr, Dobbie et al. (2006); (6) NGC 2516, 158 ± 20 Myr, Ferrario et al. (2005); (7) NGC 2168, 175 ± 25 Myr, Williams et al. (2004, 2009) (8) NGC 2287, 243 ± 40 Myr, Dobbie et al. (2009b); (9) NGC 3532, 300 ± 25 Myr, Dobbie et al. (2009b); (10) NGC 2099, 490 ± 70 Myr, Ferrario et al. (2005); (11) Coma Berenices (Melotte 111), 500 ± 100 Myr, Dobbie et al. (2009a) (12) The Hyades, 625 ± 50 Myr, Claver et al. (2005); (13) DB in the Hyades, 625 ± 50 Myr, Bergeron et al. (2011); (14) The Praesepe, 625 ± 50 Myr, Casewell et al. (2009) (15) The Praesepe, 625 ± 50 Myr, Claver et al. (2001); (16) NGC 7789, 1.4 ± 0.14 Gyr, Kalirai et al. (2008); (17) NGC 6819, 2.5 ± 0.25 Gyr, Kalirai et al. (2008); (18) NGC 6791, 8.5 ± 1 Gyr, Kalirai et al. (2007); (19) Messier 4,

~ 12.7 Gyr, Kalirai et al. (2009);

REFERENCES

- Allende Prieto, C., Asplund, M., Garcia Lopez, R.J., & Lambert, D.L. 2002, ApJ, 567, 544
- Allende Prieto, C., Barklem, P.S., Lambert, D.L., & Cunha, K. 2004, A&A, 420, 183
- Arnett, D., Meakin, C., & Young, P.A. 2009, ApJ, 690, 1715
- Arnett, D., Meakin, C., & Young, P.A. 2010, ApJ, 710, 1619
- Asplund, M., Grevesse, N., Sauval, A.J., & Scott, P. 2009, ARA&A, 47, 481 (A09)
- Asplund, M., Grevesse, N., & Sauval, A.J. 2005, in *Cosmic Abundances as Records of Stellar Evolution and Nucleosynthesis in honor of David L. Lambert*, ASP. Conf. Series, v. 336, eds. T. G. Barnes III & F. N. Bash (San Francisco: Astronomical Society of the Pacific) p. 25
- Asplund, M., Grevesse, N., Sauval, A.J., Allende Prieto, C., & Kiselman, D. 2004, A&A, 417, 751
- Aufdenberg, J.P., Ludwig, H.-G., & Kervella, P. 2005, ApJ, 633, 424
- Auwers, G.F.J.. 1862, De motu proprio Procyonis varabili
- Bahcall, J.N., Basu, S., Pinsonneault, M., & Serenelli, A.M. 2005, ApJ, 618, 1049
- Basu, S., & Antia, H.M. 2004, ApJ, 606, L85
- Barban, C., Michel, E., Martić, M., et al. 1999, A&A, 350, 617
- Bedding, T.R. et al. 2010, ApJ, 713, 935
- Bergeron, P., Kidder, K.M., Holberg, J.B., Liebert, J., Wesemael, F., & Saffer, R.A. 1991, ApJ, 372, 267
- Bergeron, P., Ruiz, M.T., & Leggett, S.K. 1997, ApJS, 108, 339
- Bergeron, P., Saffer, R.A., & Liebert, J. 2002, ApJ, 394, 228
- Bergeron, P. et al. 2011, ApJ, 737, 28

- Bessel, F.W. 1844, MNRAS, 6, 136
- Bonanno, A., Küker, M., & Paternò, L. 2007, A&A, 462, 1031
- Brown, T.M., Gilliland, R.L., Noyes, R.W., & Ramsey, L.W. 1991, ApJ, 368, 599
- Casagrande, L., Ramirez, I., Melendez, J., Bessell, M., & Asplund, M. 2010, A&A, 512, A54
- Casewell, S.L., Dobbie, P.L., Napiwotzki, R., Burleigh, M.R., Barstow, M.A., & Jameson, R.F. 2009, MNRAS, 395, 1795
- Chaboyer, B., Demarque, P., & Guenther, D.B. 1999, ApJ, 525, L41
- Chiavassa, A., Bigot, L., Kervella, P., Matter, A., Lopez, B., Collet, R., Magic, Z., & Asplund, M. 2012, A&A, 540, A5
- Claver, C.F., Liebert, J., Bergeron, P., & Koester, D. 2001, ApJ, 563, 987
- Di Mauro, M.P., & Christensen-Dalsgaard, J. 2001, IAUS 203, 94
- Dobbie, P.D., Casewell, S.L., Burleigh, M.R., & Boyce, D.D. 2009a, MNRAS, 395, 1591
- Dobbie, P.D., Napiwotzki, R., Burleigh, M.R., Williams, K.A., Sharp, R., Caswell, S.L., & Hubeny, I. 2009b, MNRAS, 395, 2248
- Dobbie, P.D., Napiwotzki, R., Lodieu, N., Burleigh, M.R., Barstow, M.A., & Jameson, R.F. 2006, MNRAS, 373, 45
- Dobbie, P.D., Pinfield, D.J., Napiwotzki, R., Hambly, N.C., Burleigh, M.R., Barstow, M.A., Jameson, R.F., & Hubeny, I. 2004, MNRAS, 355, 39
- Dogan, G., Bonanno, A., Bedding, T.R., Campante, T.L., Christensen-Dalsgaard, J., & Kjeldsen, H. 2010, AN, 331, 949
- Dufour, P., Bergeron, P., & Fontaine, G. 2005, ApJ, 627, 404
- Eggen, O.J. 1958, MNRAS, 118, 65
- Eggenberger, P., Carrier, F., & Bouchy, F. 2005, New Astron. 10, 195

- Eisenstein, D. et al. 2006, *AJ*, 132, 676
- Ferrario, L., Wickramasinghe, D.T., Liebert, J., & Williams, K.A. 2005, *MNRAS*, 361, 1131
- Fitzgerald, A.P. 1966, *Irish Astronomical Journal*, vol. vii, 213
- Fontaine, G., & Brassard, P. 2005, in the 14th European Workshop on White Dwarfs, *ASP Conf. Ser.* 334, eds. D. Koester & S. Moehler (San Francisco: ASP), p. 49
- Fontaine, G., Brassard, P., & Bergeron, P. 2001, *PASP.*, 113, 409
- Freytag, B., Steffen, M., & Dorch, B. 2002, *Astron. Nachr.*, 323, 213
- Gatewood, G. 1987, *AJ*, 94, 213
- Gatewood, G. & Han, I. 2006, *AJ*, 131, 1015
- Ghoul, A.A., Bahcall, J.N., & Loeb, A. 1994, *ApJ*, 421, 828
- Girard, R.M., et al. 2000, *AJ*, 119, 2428
- Grevesse, N., & Sauval, A.J. 1998, *Space Science Reviews*, v. 85, p. 161
- Guenther, D.B., & Demarque, P. 1993, *ApJ*, 405, 298
- Hansen, B.M.S. 1999, *ApJ*, 520 680
- Hansen, B.M.S. et al. 2002, *ApJ*, 574, L155
- Hansen, B.M.S. et al. 2007, *ApJ*, 671, 380
- Harrington, R.S., Christy, J.W., & Strand, K.A. 1981, *AJ*, 86, 909
- Hauschildt, P.H., Allard, F., Ferguson, J., Baron, E., & Alexander, D.R. 1999, *ApJ*, 525, 871
- Henry, T.J.. 2011, in *Observer's Handbook 2011*, ed. P. Kelly, (The Royal Astronomical Society of Canada: Toronto) p. 293
- Heiter, U. & Luck, R.E. 2003, *AJ*, 126, 2015

- Holberg, J.B. 2009, *J. Hist. Astr.*, 40, 137
- Iben, I.Jr. 1984, *ApJ*, 277, 333
- Irwin, A.W., Fletcher, J.M., Yang, S.L.S., Walker, G.A.H., & Goodenough, C. 1992, *PASP*, 104, 489
- Kalirai, J.S., Bergeron, P., Hansen, B.M.S., Kelson, D.D., Reitzel, D.B., Rich, R.M., & Richer, H.B. 2007, *ApJ*, 671, 748
- Kalirai, J.S., Saul Davis, D., Richer, H.B., Bergeron, P., Catelan, M., Hansen, B.M.S., & Rich, R.M. 2009, *ApJ*, 705, 408
- Kalirai, J.S., Hansen, B.M.S., Kelson, D.D., Reitzel, D.B., Rich, R.M., & Richer, H.B. 2008, *ApJ*, 676, 594
- Kalirai, J.S., Richer, H.B., Reitzel, D., Hansen, B.M.S., Rich, R.M., Fahlman, G.G., Gibson, B.K., and von Hippel, T. 2005, *ApJ*, 618, L123
- Kervella, P., Thevenin, F., Morel, P., Berthomieu, G., Borde, P., & Provost, J. 2004, *A&A*, 413, 251
- Koester, D., & Reimers, D. 1993, *A&A*, 275, 479
- Koester, D., Schulz, H., & Weidemann, V. 1979, *A&A*, 76, 262
- Kurucz, R.L. 1992, *Rev. Mex. AA*, 23, 187
- Liebert, J., Dahn, C.C., & Monet, D.G. 1988, *ApJ*, 332, 891
- Liebert, J., Young, P.A., Arnett, D., Holberg, J.B., & Williams, K.A. 2005, *ApJ*, 630, L69 (Paper I)
- Lodders, K. 2010, “Solar System Abundances of the Elements”, in *Principles and Perspectives in Cosmochemistry, Astrophysics & Space Sciences Proceedings*, vol. ISBN 978-3-642-10351-3 (Berlin Heidelberg: Springer-Verlag), p. 379

- Luck, R.E., & Heiter, U. 2005, AJ, 129, 1063
- Mozurkewich, D. et al. 1991, AJ, 101, 2207
- Mucciarelli, A., Salaris, M., Lovisi, L., Ferraro, F.R., Lanzoni, B., Lucatello, S., & Gratton, R.G. 2011, MNRAS, 412, 81
- Nordström, B., Mayor, M., Andersen, J., Holmberg, J., Pont, F., Jørgensen, B.R., Olsen, E.H., Udry, S., & Mowlavi, N. 2004, A&A, 418, 989
- Provencal, J.L., Shipman, H.L., Koester, D., Wesemael, F., & Bergeron, P. 2002, ApJ, 568, 324
- Provencal, J.L., Shipman, H.L., Wesemael, F., Bergeron, P., Bond, H.E., Liebert, J., & Sion, E.M. 1997, ApJ, 480, 777
- Provost, J., Berthomieu, G., Martič, M., & Morel, P. 2006, A&A, 460, 759
- Salaris, M., Dominguez, I., Garcia-Berro, E., Hernanz, M., Isern, J., & Mochkovitch, R. 1997, ApJ, 486, 413
- Schaefer, G.H., Bond, H.E., Barstow, M.A., Burleigh, M., Gilliland, R.L., Girard, T.M., Gudehus, D.H., Holberg, J.B., & Nelan, E. 2006, BAAS, 38, 1104
- Shipman, H.L., & Provencal, J.L. 1999, in *White Dwarfs*, 11th European Workshop on White Dwarfs, eds. J.-E. Solheim & E.G. Meistas (San Francisco: ASP), p. 15
- Strand, K.A. 1951, ApJ, 113, 1
- Sung, H., & Bessell, M.S. 1999, MNRAS, 306, 361
- Tassoul, M., Fontaine, G., & Winget, D.E. 1990, ApJS, 72, 335
- Valenti, J.A., & Fischer, D.A. 2005, ApJS, 159, 141
- van Leeuwen, F. 2007, A&A, 474, 653
- von Hippel, T. 2005, ApJ, 622, 565

Williams, K.A., Bolte, M., & Koester, D. 2004, *ApJ*, 615, L49

Williams, K.A., Bolte, M., & Koester, D. 2009, *ApJ*, 693, 355

Wood, M.A. 1992, *ApJ*, 386, 539

Wood, M.A. 1995, in *White Dwarfs*, eds. D. Koester & K. Werner (Berlin: Springer), p. 41

Young, P.A., & Arnett, D. 2005, *ApJ*, 618, 908

Young, P.A., Mamajek, E., Arnett, D., & Liebert, J. 2001, *ApJ*, 556, 230

Zuckerman, B., & Song, I. 2004, *ARA&A*, 42, 685

FIGURE CAPTIONS

Fig. 1 — TYCHO evolutionary tracks in a log luminosity vs. log radius diagram beginning including the pre-main sequence at the Asplund, Grevesse, & Sauval (2005, 2009 =A09) primordial solar abundance of $Z=0.0122$ for masses of (in descending order of luminosity) $1.499 M_{\odot}$ (black), the favored preliminary HST astrometric value, $1.48 M_{\odot}$ (red), the best fit to the observed luminosity, $1.463 M_{\odot}$ (green), and $1.42 M_{\odot}$ (blue).

Fig. 2 — The initial to final mass relation (IFMR) for Procyon B, Sirius B and the white dwarfs in a number of star clusters discussed in the text. Procyon B and Sirius B (from Paper I) are plotted as black, filled circles. The total data set for older open clusters from Kalirai et al. (2007, 2008, 2009) are also plotted with filled symbols – NGC 7789 (red), NGC 6819 (green), NGC 6791 (blue) and Messier 4 (magenta). Shown with open circles – taken from Ferrario et al. (2005) and Paper I – are the Pleiades (red), NGC 2516 (cyan), NGC 2168 (magenta), the Hyades (blue) and Praesepe (cyan), NGC 3532 (green), and NGC 2099 (yellow). The error bars include the best estimates of the cluster ages. The magenta line plots the simple linear relation from Ferrario et al. (2005). The Procyon B remnant mass appears low relative to the others, as discussed in the text.

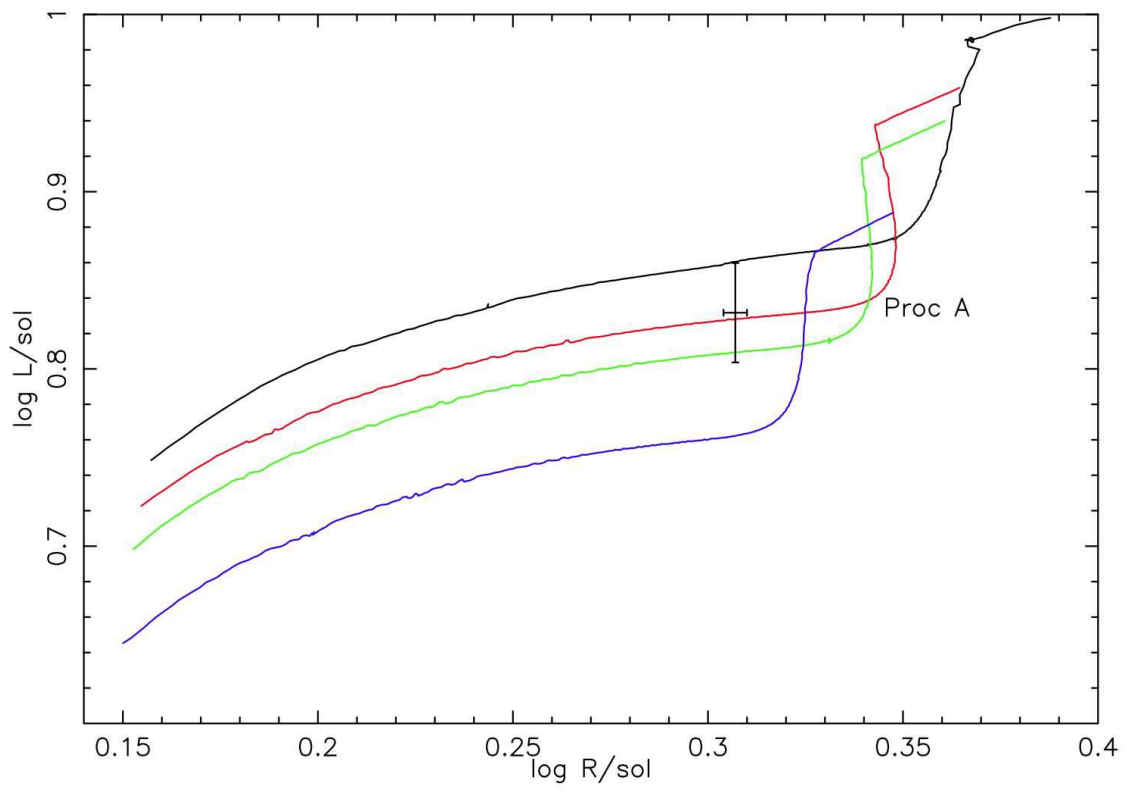


Figure 1

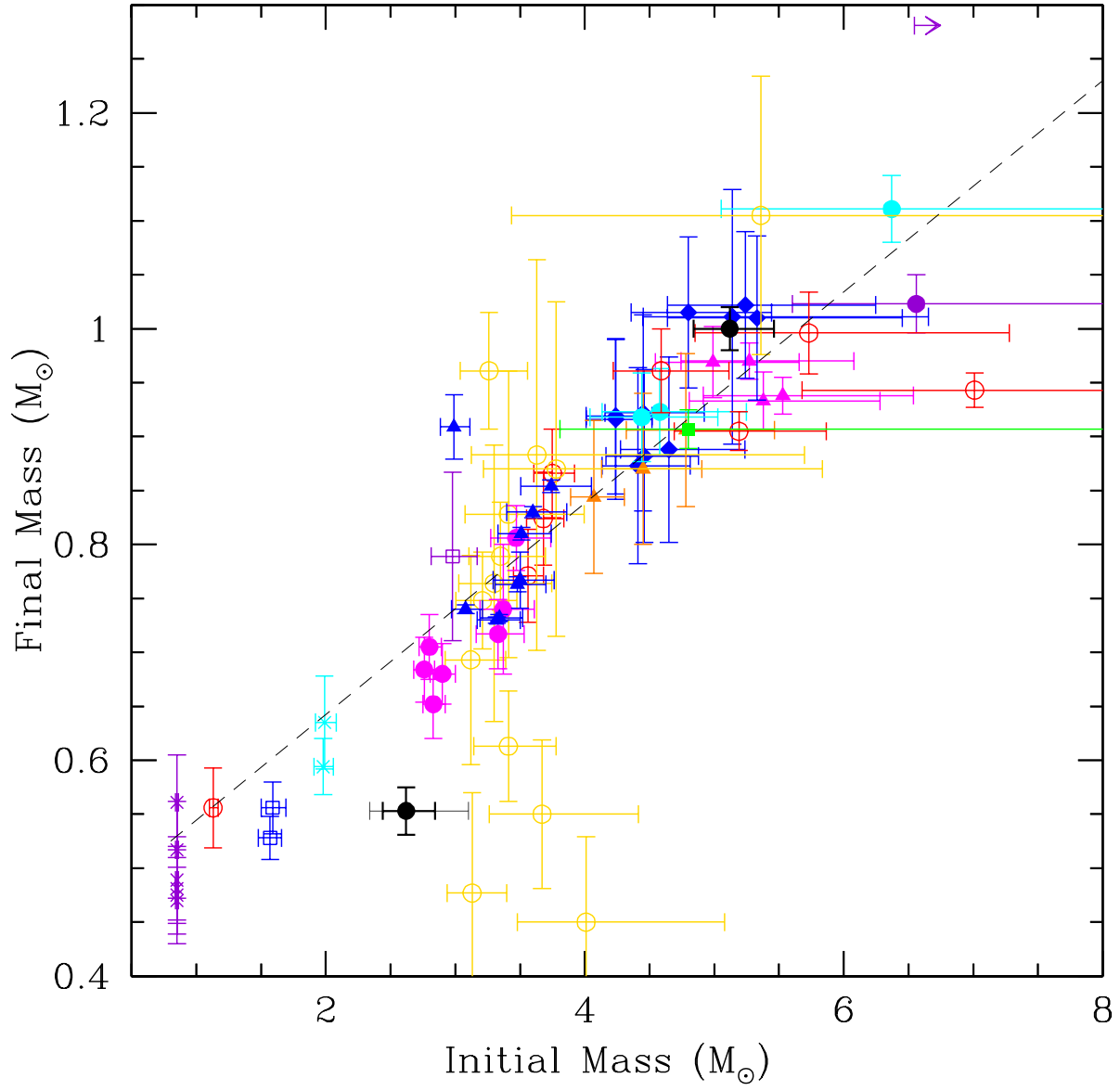


Figure 2